ENHANCING VIBRATION STABILITY IN END-FACE TRIMMING USING WIDE-BLADED CUTTERS

Olexandr Badovskyi[1] [0009-0008-1607-4078], Anna Balaniuk[1] [0000-0003-1628-0273], Gennadii Oborskyi[1] [0000-0002-5682-4768], Alexandr Orgiyan[1] [0000-0002-1698-402X], Vitalii Ivanov[2,3,4] [0000-0003-0595-2660]
[1]Odesa Polytechnic National University, 1, Shevchenko Avenue, Odesa 65044, Ukraine
[2]Sumy State University, 116, Kharkivska St., Sumy 40007, Ukraine
[3]Technical University of Košice, 1, Bayerova St., Prešov 080 01, Slovak Republic
[4]WSB University, 1C, Ciplaka St., Dabrowa Gornicza 41-300, Poland
E-mail(s): ivanov@tmvi.sumdu.edu.ua(✉) (corresponding author's e-mail), *badovskyi.8111276@stud.op.edu.ua, balanuk.a.v@op.edu.ua, oborsky@op.edu.ua, orgiyan.a.a@op.edu.ua*

Abstract - Trimming the ends of parts using wide-bladed cutters is a simple and highly productive technological operation, often performed on finishing and boring machines (FBM). However, the use of this operation for parts with significant end widths is limited by vibrations caused by insufficient rigidity of the fixture clamping the workpiece. For the first time, the dynamics of trimming free and internal ends with wide-bladed cutters under axial feed have been studied, revealing the dominant role of the fixture's rigidity in ensuring the vibration stability of the technological system. It has been established that the natural vibration frequencies of the fixtures (90–180 Hz) are half those of the spindle heads (300–400 Hz). Therefore, the loss of stability in such technological systems is primarily determined by the fixture's elastic system parameters. Furthermore, the vibration stability of FBM during internal turning was investigated by combining fine boring and trimming operations. In this case, the tip of the wide-bladed cutter bored a cylindrical hole, while the main cutting edge, made in the form of a rectangular wide blade, machined the internal end face. The formulation and solution of these technological problems provide a highly convenient approach for studying the vibrations of systems with variable parameters, as they account for changes in the position of the cutting zone. Based on these experiments, the article describes a developed method for solving vibration resistance issues in FBM when cutting the ends of parts made of plastic and brittle materials. Ultimately, the study determines the requirements for the rational design of fixtures and guidelines for selecting cutting modes to prevent vibrations during the machining of the corresponding parts.

Keywords: Axial Feed, Closed Dynamic System, Wide-Bladed Cutter, Frequency Response, Rigidity, Fixture, Boring, Industrial Growth.

1. Introduction

When trimming the ends of parts, the main focus is on high quality and optimal productivity. Two methods are often used in machining: radial feed and axial feed. The axial feed (cutting) method is simpler and more productive, but less studied. To assess the feasibility of the axial feed method, theoretical and experimental studies of the dynamic interactions between the "spindle-bar" and "part-fixture" subsystems during free and internal-end-face turning were conducted. The features of dynamic interactions when combining thin boring with internal end face undercutting were studied.

It is known that the stability of turning and milling processes is largely determined by the dynamic characteristics of the technological system, such as stiffness, damping, and frequency characteristics in the cutting zone [1, 2]. At the same time, when machining with small cutting thicknesses and wide cutting edges, the influence of unsteady cutting forces and regenerative effects increases,

dx.doi.org/10.17683/ijomam/issue24.4

potentially leading to self-oscillations [3]. Numerous studies show that the parameters of the "part-fixture" subsystem often have a decisive influence on vibration resistance relative to the "spindle-tool" subsystem [4, 5]. Despite the development of analytical, mechanistic, and numerical cutting models [6, 7, 8], issues of vibration resistance in end-face trimming operations with axial feed remain insufficiently studied, especially when combined with thin-boring of internal surfaces [9].

Unlike existing studies that focus on the dynamics of spindle units, this research, for the first time, reveals the determining role of the "part-fixture" system's compliance in operations involving trimming ends with wide-bladed cutters. The scientific novelty of the work lies in establishing patterns of change in vibration stability under variable cutting-zone position during axial feed, as well as changes in the direction of the cutting forces acting on the cutter.

This work aims to improve the vibration stability of a non-stationary technological system during the turning and undercutting of the free and internal ends of parts using wide-bladed cutters.

To achieve this goal, the following tasks have been set:

1. Determine the features of the dynamic characteristics of the cutting process during the trimming of the ends of parts made of plastic and brittle materials.

2. Determine the characteristics of dynamic interactions when combining boring operations with end trimming.

3. Develop recommendations for determining the maximum width of the ends permissible according to the cutting process stability condition.

2. Literature Review

The dynamics of machining processes, the prediction of cutting forces, and the vibration resistance of technological systems are key issues in modern mechanical engineering, as they directly affect the accuracy, surface quality, and productivity of machining. These issues are particularly relevant in fine turning, end-face trimming, and the machining of parts with reduced rigidity.

One of the fundamental areas of research is the virtualization and modeling of machine tool dynamics. Study [1] presents the concept of a "virtual machine tool," which enables evaluation of the static rigidity, natural vibration modes, and frequency characteristics at the tool's central point. The proposed approach enables replacing labor-intensive experimental tests with numerical analysis to investigate the stability of milling and turning processes.

Mechanistic models of cutting forces have undergone significant development. The unified model proposed in [6] enables predicting forces for various machining operations (turning, boring, drilling, milling) by reducing the loads acting on the cutting edge to a single coordinate system.

In the field of orthogonal cutting, significant contributions have been made by researchers in [10] and [11], who predict cutting forces using micromechanical models and experimentally identified cutting coefficients. Such models allow both the shear and the displacement (ploughing) components of the force to be considered, which is extremely important when removing thin chips.

Analytical thermomechanical models of oblique cutting were developed in the study [7], which applied them to peripheral milling of titanium alloys. The proposed three-dimensional model of cutting forces considers strain hardening, thermal softening, and inertial effects.

The identification of cutting force coefficients for linear and nonlinear end-milling models is discussed in the study [12]. The authors showed that the methods of mean force s and optimization provide sufficient reproduction of experimental results, which is important for further analysis of vibration stability. An analysis of recent studies shows that the surface layer condition and the tribological properties of contact pairs significantly affect the wear resistance and stability of mechanical interactions in cutting processes, as confirmed by experimental results for the steel-cast iron pair under dry friction conditions [13]. Friction conditions in the cutting zone, including those with minimal lubrication, determine the level of specific cutting energy and the intensity of tool wear [14].

Numerical methods, in particular the finite element method (FEM), are widely used to study cutting processes. Works [8, 15, 16] show that FEM allows for a detailed study of the influence of tool geometry, large negative rake angles, friction conditions, and minimal lubrication on cutting forces, wear, and thermal processes.

A separate area of research is the development of prediction methods based on artificial intelligence. In works [17, 18, 19] and [20], the effectiveness of neural networks and genetic algorithms for predicting cutting forces and surface roughness, and for optimizing machining modes, has been demonstrated. Functional dependencies between the cutting process parameters and the surface layer quality criteria have been established [21].

Several studies have examined vibration and cutting along a track. Analytical modeling of the dynamics of the "spindle-tool" system based on Timoshenko's beam theory is presented in [2], which is the basis for constructing stability diagrams. Modern methods for recording vibrations using wavelet transforms and SVM algorithms are proposed in [22].

A special group comprises studies on the machining of thin-walled, low-rigidity parts. Research [4] and [5] considers the influence of

variable stiffness and deformations induced by cutting forces, as well as methods to compensate for the resulting errors.

When performing fine turning and end-face cutting, it is important to understand the dynamics of the cutting process at low chip thicknesses. Research [3] laid the foundation for a dynamic description of the turning process that accounts for regenerative effects and damping. The works of [23] and [9] directly analyze the vibration resistance of finishing operations and end trimming, demonstrating the decisive role of the "part-fixture" subsystem's stiffness. Changes in the spindle speed also determine the energy efficiency of face turning. Accounting for this factor in integrated models reduces total energy losses [24].

Thus, the literature review shows that while the issues of predicting cutting forces and the dynamics of machining processes have been studied extensively, the task of vibration stability during the trimming of the ends of plastic and brittle materials with wide-bladed cutters on FBM, considering the variable stiffness of the fixtures, remains relevant.

3. Research Methodology

Specimens made of steel and cast iron were used in the study; the diameters of the trimmed ends were varied from 40 to 100 mm, and their widths from 4 to 10 mm. The cutting forces and phase shift between the force and the displacement x were measured when the device was excited by a vibrator over the frequency range from 20 to 600 Hz. The cutting speed ranged from 0.83 to 2.50 m/s, the width of the free end being cut was 0.5–4.0 mm, and the feed was 0.01–0.04 mm/rev.

As the measuring equipment, a device for recording vibrations was used. This device consists of 4 strain gauges connected in a bridge circuit, a Discovery STM32L0538-DISCO microcontroller, a strain gauge amplifier, a microSD memory card, and a Bluetooth radio module. A specific feature of this design is that the signal is recorded not by a PC but directly by the Discovery STM32L0538-DISCO microcontroller, which is controlled by a computer via Bluetooth. The device was calibrated based on the magnitude of the boring bar's static displacement in the cutter cross-section.

When cutting steel C45 (EN), cutters with P01 (EN ISO 513) alloy inserts with the following geometry were used: α=9º, γ=15º, λ=0º; When undercutting the ends of EN-GJL-150 (EN) workpieces, cutting inserts made of K01(EN ISO 513) alloy with the following geometry were used: α=9º, γ=5º. The rigidity of the fixture was also varied in the experiments.

The system's approximation to the limit state of stability was determined by the oscillation amplitudes during cutting and during idle running (Acut/Aidle). It is known that during boring, the limit values of the parameters can be taken to correspond to the ratio $A_{cut}/A_{idle} = 1.5$ [9].

The diagram of processing the ends of a part with a wide-bladed cutter is shown in Fig. 1.

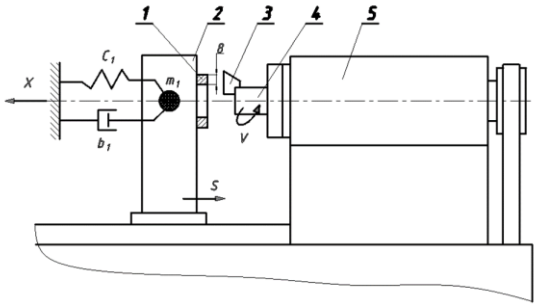

Figure 1: Diagram of machining the ends of a workpiece with a wide-bladed cutter

When performing the undercutting operation, workpiece 1 is clamped in fixture 2, which is mounted on the machine tool's movable table. Cutter 3, whose cutting-edge length exceeds the width of the undercut end Bpr, is fixed in the side bar 4 installed on the spindle head 5. The vibrations arising during the cutting process are mainly oriented relative to the normal to the machined surface. They are determined by the coordinate *x*, along which the cutting force $P_{(x)}$ acts.

Below is a description of a calculation method based on special experiments for solving the problem of vibration stability during FBM undercutting of the ends of parts made of plastic and brittle materials with a wide-bladed cutter.

4. Results

The dynamic system describing vibrations during end trimming can be represented as two elastic subsystems that interact during the cutting process. The differential equations of motion of the elastic subsystems "spindle-tool" and "part-fixture" are as follows:

$$\begin{aligned} m_1\ddot{x}_1 + b_1\dot{x}_1 + c_1x_1 &= \mu P_z, \\ m_2\ddot{x}_2 + b_2\dot{x}_2 + c_2x_2 &= \mu P_z, \end{aligned} \quad (1)$$

where $\mu P_z = P_x$; μ – coefficient of friction of the chip relative to the front edge of the cutter; m_1, m_2 – masses reduced to the cutting zone; b_1, b_2 – damping coefficients;

c_1, c_2 – stiffnesses; x_1, x_2 – elastic displacements of subsystems.

Note that the stiffness of the spindle heads varies from 200 to 500 MN/m, while the stiffness of the

devices used for end trimming varies from 80 to 120 MN/m. The frequencies of free vibrations of the spindle heads along their axes are approximately 400 Hz, and the frequencies of the fixtures' vibrations are 100–180 Hz. Based on this comparison, it can be concluded that only the vibrations of the "part-fixture" subsystem should be taken into account in the calculation model, as it is more compliant and has no frequency content. Mutual movements of the part and tool $x = x_1 - x_2 \approx x_1$.

To describe the cutting process when machining plastic materials, we use the dynamic characteristics of the cutting process.

$$T_p \dot{P}_z + P_z = -k_p \left[x + \left(T_\alpha - T_\gamma \right) \dot{x} + T_\alpha T_p \ddot{x} \right] \qquad (2)$$

This type of characteristic describes changes in cutting force as a function of displacement along the x-axis. The time constants P_γ, as well as cutting rigidity k_p, are determined based on the known characteristics of the material being machined, the tool, and the machining mode. It is known that when removing thin chips with a sharp cutter, the chip formation time constant P_p significantly exceeds P_α and P_γ, therefore, the cutting process characteristic can be simplified [9]:

$$T_p \dot{P}_z + P_z = -k_p x \qquad (3)$$

The dynamic characteristics of the cutting process during the machining of brittle materials have not been studied previously. Therefore, an experiment was conducted to determine the frequency characteristics of turning cast iron. Based on the measurement results, amplitude-phase frequency characteristics (APFC) were constructed for cast iron and steel (Fig. 2). The approximation curves for steel are similar to those for cast iron.

As shown, at a given disturbance frequency, the phase shift decreases with increasing cutting speed. Therefore, at cutting speeds of about 2.5 m/s and frequencies in the 600–800 Hz range, which includes the system's maximum frequencies, the experimental data can be approximated by the simplest characteristic of the cutting process (3). When the cutting speed is reduced to 0.83 m/s, the results should account for the time constant's influence T_α. The experimental data obtained allow us to conclude that for calculating vibration resistance when cutting brittle materials, as well as for plastic materials, dynamic characteristic (3) or (2) can be used.

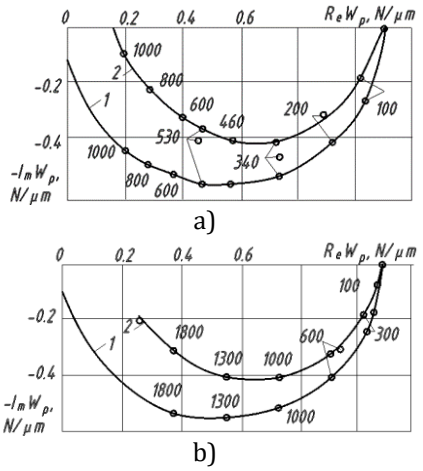

Figure 2: Calculated and experimental APFC, s = 0.02 mm/rev: a) v = 0.8; b) v = 2.5

Equations (1) form a system whose stability can be investigated using frequency or algebraic criteria. The above features of the system allow us to judge its stability based on the results of solving equations (1) and (3). The stability condition in this case is as follows:

$$m_1 b_1 + b_1 T_p \left(b_1 + c_1 T_p \right) - k_p \mu m_1 T_p > 0 \qquad (4)$$

This equation enables the calculation of the tool parameters (stiffness, damping, reduced mass) and the cutting process (speed, feed, workpiece end-face width), ensuring stable machining. For example, to calculate the maximum width of the cut end face, equation (4) is transformed as follows:

$$B_{pr} = \frac{m_1 b_1 + b_1 T_p \left(b_1 + c_1 T_p \right)}{1,5 \sigma_b \xi \mu m_1 T_p} \qquad (5)$$

where σ_b is the tensile strength of the material being machined; ξ is the chip shrinkage.

The correctness of the obtained expression (5) was verified by comparing the calculated and experimental values B_{pr} of as a function of the parameters of the elastic system of the special device. Using this method for trimming allows for comparing the results of calculations and experiments.

Fig. 2b shows the stability zone as the cut-end width of the part is varied and the compliance K of the elastic system of the fixture during machining of steel blanks. Changing the material being machined and the cutting conditions does not distort the established dependencies.

It has been established that when the cutter angle λ is reduced from 10° to 0°, the system's vibration stability increases. When machining large-diameter ends, significant changes in the fixture's compliance

within the range of rotation are accompanied by corresponding changes in the vibration level.

The process of removing thin chips differs significantly from conventional machining in that the small size of the cut layer ultimately affects several important process characteristics: chip shrinkage, the friction coefficient between the chip and the cutter, specific cutting force, and the decomposition of the cutting force into components.

Let us consider some features of determining the components of cutting force in thin turning. Due to the small cutting depth, the cutter primarily operates with its tip, and the curved portions of the main and auxiliary cutting edges contact the workpiece.

Therefore, during fine boring, the simplest relationships between the components of the total cutting force, defined for "normal chips" (Fig. 3), do not apply.

Fig. 3 considers only the forces acting on the front surface of the cutter, the resultant of which is N. The coefficient characterizes changes in the friction between the chips and the front edge.

$$\begin{aligned} P_z &= N\left(\cos\gamma + \mu\sin\gamma\right), \\ P_{xy} &= N\left(-\sin\gamma + \mu\cos\gamma\right), \\ P_y &= P_{xy}\cos\varphi, \\ P_x &= P_{xy}\sin\varphi. \end{aligned} \tag{6}$$

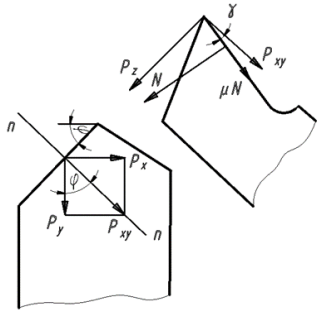

a)

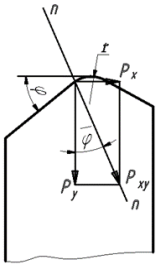

b)

Figure 3: Diagrams for determining cutting forces: a) sharp-edged cutter, b) thin-boring cutter

The ratios (6) are simplified for small or zero values of the front angle of the cutter γ:

$$P_z = N, P_{xy} = \mu P_z \tag{7}$$

The decomposition of the components P_{xy} into components P_x and P_y during thin boring depends not only on the angle φ, but also on the value of the radius at the tip r and the dimensions of the cutting section. The direction n of the force P_{xy} forms an angle $\bar{\varphi}$ with the axis y. Physically, the angle $\bar{\varphi}$ is a certain effective value of the main angle φ in the plane of the cutter removing thin chips. Introducing this angle allows us to write expressions for the cutting force components:

$$\begin{aligned} P_y &= P_{xy}\cos\bar{\varphi}, \\ P_x &= P_{xy}\sin\bar{\varphi}, \\ \bar{\varphi} &= \operatorname{arc}tg\frac{P_x}{P_y}. \end{aligned} \tag{8}$$

Experiments have shown that the angle $\bar{\varphi}$ differs significantly from the angle φ. Thus, the angle $\bar{\varphi}$ reflects the unevenness of the deformations of the cut metal on the curved part of the blade.

The experimental setup for studying the combination of fine boring and undercutting of internal ends is shown in Fig. 4a, while Fig. 4b shows the cutter angles in the cutting zone.

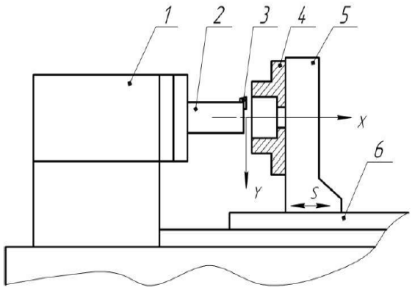

a)

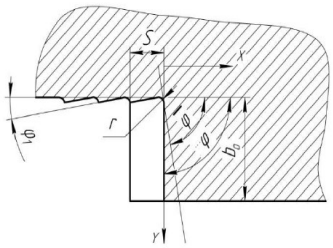

b)

Figure 4: Experiment diagram a) and cutter angles in the cutting zone b)

For the computational model of boring with undercutting, the associated vibrations in the radial (y-axis) and axial (x-axis) directions were considered.

Therefore, the characteristics of the "spindle–boring bar" and "fixture–workpiece" subsystems are determined by the masses (m_y and m_z), reduced to the cutter stiffnesses (c_y and c_x) and damping parameters (b_y and b_x) at vibrations at natural frequencies (f_y and f_x).

In a closed dynamic model, the connection between the vibrations of these two subsystems arises through the cutting process. For the cutting process, we use the dynamic characteristic [14], which describes the lag of the cutting force P_z behind changes in the cut thickness a.

$$T_p \dot{P}_z + P_z = -k_p a \tag{9}$$

where $T_p = 1,5\frac{a_0 \xi}{V}$ is the chip formation time constant (a_0 is the chip thickness, ξ is the maximum chip shrinkage, and V is the cutting speed); $k_p = 1,5\sigma_0 \xi b_0$ is the cutting coefficient (σ_0 is the time resistance, b_0 is the cutting width).

When there are fluctuations along the u and x axes in the cutting zone, the cutting thickness a change. The change in cutting thickness can be described as the sum of two displacements in the direction of chip flow, perpendicular to the side of the angle $\bar{\varphi}$. Note that in non-free cutting, the angle $\varphi > \bar{\varphi}$, and in free cutting, $\varphi = \bar{\varphi}$.

The change in the thickness of the cut layer can be expressed as follows:

$$a = y\cos\bar{\varphi} + x\sin\bar{\varphi}. \tag{10}$$

The equations of motion of the dynamic system are as follows:

$$\begin{aligned} m_y \ddot{y} + b_y \dot{y} + c_y y &= P_y, \\ m_x \ddot{x} + b_x \dot{x} + c_x x &= P_x. \end{aligned} \tag{11}$$

For small forward angles γ, we can assume

$$P_{xy} = \mu P_z,$$
$$P_x = P_{xy}\sin\bar{\varphi},$$
$$P_y = P_{xy}\cos\bar{\varphi}.$$

After substituting these ratios into equations (11) and (10) into equation (6), we obtain an equation close to the cutting process of an elastic system:

$$\begin{aligned} m_y \ddot{y} + b_y \dot{y} + c_y y &= P_z \mu\cos\bar{\varphi}, \\ m_x \ddot{x} + b_x \dot{x} + c_x x &= P_z \mu\sin\bar{\varphi}, \\ T_p \dot{P}_z + P_z &= -k_p \left(y\cos\bar{\varphi} + x\sin\bar{\varphi}\right). \end{aligned} \tag{12}$$

It is important to note that with thin end cutting, the effective angle $\bar{\varphi}$ differs little from π/2. Denoting the small angle $\psi = \frac{\pi}{2} - \bar{\varphi}$, we write the expressions of the functions from the argument $\bar{\varphi}$:

$$\sin\bar{\varphi} \approx 1 - \frac{\psi^2}{2},$$
$$\cos\bar{\varphi} \approx \psi.$$

Equations (12) can be represented as:

$$\begin{aligned} m_y \ddot{y} + b_y \dot{y} + C_y y &= P_z \mu\psi, \\ m_x \ddot{x} + b_x \dot{x} + C_x x &= P_z \mu\left(1 - \frac{\psi^2}{2}\right), \\ T_p \dot{P}_z + P_z &= -k_p \left[y\psi + x\left(1 - \frac{\psi^2}{2}\right)\right]. \end{aligned} \tag{13}$$

Neglecting the terms with ψ^4, we write the characteristic equation for the system (13)

$$\begin{aligned} &\left(m_y p^2 + b_y p + C_y\right)\left(m_x p^2 + b_x p + C_x\right)\left(T_p p + 1\right) + \\ &+ \mu k_p \psi^2 \left(m_x p^2 + b_x p + C_x\right) + \mu k_p \left(1 - \psi^2\right)\left(m_y p^2 + b_y p + C_y\right) = 0. \end{aligned}$$

Noting that all coefficients of this equation are positive, the closed dynamic system will be stable if two conditions are met:

$$\Delta_2 = \left(a_1 a_2 - a_0 a_3\right) \succ 0,$$
$$\Delta_4 = \Delta_2\left(a_3 a_4 - a_2 a_5\right) - \left(a_1 a_4 - a_0 a_5\right)^2 \succ 0,$$

where:

$$a_0 = m_y m_x T_p,$$
$$a_1 = m_y m_x + T_p\left(m_y b_x + m_x b_y\right),$$
$$a_2 = T_p\left(m_y C_x + m_x C_y + b_x b_y\right) + m_y b_x + m_x b_y,$$
$$a_3 = T_p\left(b_y C_x + b_x C_y\right) + m_y C_x + m_x C_y + b_x b_y + \mu k_p \psi^2 m_x + \mu k_p\left(1 - \psi^2\right) m_y,$$
$$a_4 = T_p C_y C_x + \left(b_y C_x + b_x C_y\right) + \mu k_p \psi^2 b_x + \mu k_p\left(1 - \psi^2\right) b_y,$$
$$a_5 = C_y C_x + \mu k_p \psi^2 C_x + \mu k_p\left(1 - \psi^2\right) C_y.$$

The calculation scheme of the closed dynamic system when combining the under-cutting and boring operations described above reflects the main feature of the system – the small difference between the angle $\bar{\varphi}$ and π/2. Therefore, the ratio P_x/P_z is large, and the oscillations in the system primarily manifest as device bending.

To determine the total technological rigidity in the feed direction and to identify the role of the fixture in the overall rigidity balance, the following were measured:

1) the relative displacements of the spindle flange and the fixture at a height of 340 mm from the table surface (Fig. 5a);

2) the displacements of the fixture relative to the table at heights of 180 mm and 340 mm from the table surface (Fig. 5b).

Loading was carried out using a jack through a compression dynamometer positioned between the flange and the fixture. The force was increased stepwise from 50 kg to 150 kg. The displacements were measured using a microcator with a graduation of 0.2 μm. The microcator was mounted on a rigid base.

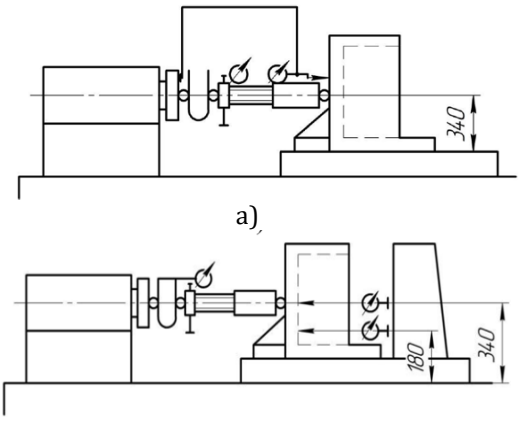

Figure 5: Measurement of static rigidity: a) of the spindle flange and the fixture, and b) of the fixture relative to the table.

Calculations of vibration resistance were performed to determine the fixture's flexibility when trimming the ends of steel and cast-iron workpieces. Rational values for fixture flexibility were determined to obtain optimal end-width values for stable cutting. Some results of the experiments and calculations are shown in Fig. 6.

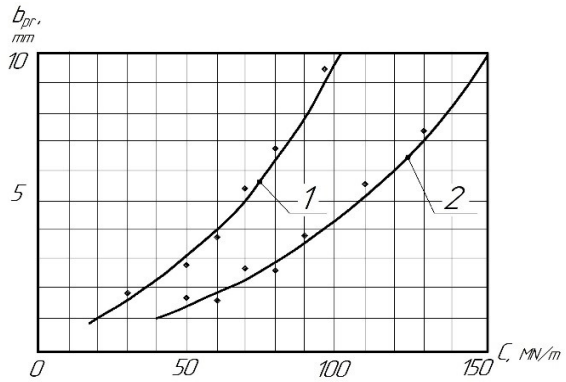

Figure 6: Limit values of the cut width for normalized fixtures 1 – EN-GJL-150 (EN); 2 – steel C45 (EN), points – experiment, curve – calculation.

The results obtained are in good agreement with modern ideas about the dynamics of cutting processes and the role of elastic subsystems in the technological system. As shown in [1, 6], the stability of turning processes is largely determined by the ratio of stiffnesses and natural frequencies of the system elements, and regenerative effects are particularly enhanced at small cutting thicknesses and wide cutting edges.

5. Discussion

Discussion of experimental results on parameter variability when turning ends of different diameters on models with variable fixture stiffness reveals patterns of change in vibration stability during undercutting. The fixtures used in FBM for basing parts with undercut ends are often box-like structures reinforced with stiffening ribs.

The dominant influence of the "part-fixture" subsystem identified in this work confirms the conclusions in [4] and [5], according to which, when machining parts with reduced rigidity, it is often the fixture that is the limiting factor in vibration resistance, even with high rigidity of the spindle assemblies [9].

The observed similarity of dynamic characteristics when cutting ductile and brittle materials is consistent with the results of works [3] and [23], which show that during thin cutting and at high speeds, the influence of the chip formation time constant decreases, and the process can be described by simplified dynamic characteristics. This confirms the possibility of using a single calculation model to assess vibration resistance when cutting the ends of parts made of different materials.

It has been established that the geometry of the cutting tool, in particular the rake angle and the lead angle, has a significant influence on the magnitude of the main cutting force component [25].

The nature of the oscillations when trimming ends of different diameters also corresponds to known ideas about systems with variable parameters. When trimming the ends of parts with diameters of about 15 mm near the stability boundary, oscillations develop whose frequency is approximately equal to that of the elastic system [2]. These oscillations have practically the same amplitude within one revolution, and there are almost no traces of oscillations visible on the ends, which are evenly distributed over the machined surface.

When cutting ends with diameters greater than 40 mm, vibrations of variable amplitude are clearly visible, with a distinct maximum when the cutter is removed from the fixture. At the same time, traces of intense vibrations are clearly visible. These vibrations have low frequencies near the spindle rotation frequency and amplitudes of about 0.3–0.4 μm. As the diameter of the end face increases, low-frequency oscillations with variable amplitude appear, synchronized with the spindle rotation, as previously noted when machining thin-walled and large-sized parts [4, 22].

Thus, the results of this study not only confirm the known provisions of cutting dynamics theory but also extend them to the operations of undercutting free and internal ends with wide-bladed cutters. The obtained dependencies enable a reasonable selection of fixture parameters and cutting modes to ensure

stable, high-quality machining on finishing and boring machines.

6. Conclusions

As a result of the theoretical and experimental studies conducted, the patterns of vibration stability during trimming of free and internal ends with wide-bladed cutters on finishing and boring machines have been established for the first time.

Furthermore, it has been established that the variability of the dynamic system parameters, driven by changes in the cutting zone position and fixture flexibility, often decisively influences the stability of the end-trimming process. This is particularly evident when machining large-diameter ends, where the effective stiffness of the "part-fixture" subsystem changes during a single revolution of the part.

The similarity of the dynamic characteristics of the cutting process during the machining of ductile and brittle materials has been experimentally confirmed. Based on a comparison of the amplitude-phase frequency characteristics obtained during the fine turning of steel and cast iron under forced-vibration conditions, it is shown that at cutting speeds of about 2.0–2.5 m/s, the dynamic characteristics of the cutting process for both materials can be described by a simplified model.

An analysis of the parameters of spindle assemblies and standardized fixtures used for end trimming with wide-bladed cutters on FBM shows that the axial rigidity of spindle assemblies (400–500 MN/m) is 3–4 times greater than the axial rigidity of the fixtures in the feed direction. Moreover, the vibration frequencies of the fixtures (90–180 Hz) are half those of the spindle heads (300–400 Hz). Therefore, the relative movements of the workpiece and tool are mainly determined by the movements of the "part-fixture" subsystem.

The minimum permissible axial rigidity of fixtures required to ensure stable trimming of the ends of steel and cast-iron parts has been experimentally established. It has been shown that when the width of the trimmed free end is up to 6 mm, the axial rigidity of the fixture must be at least 200 N/μm. It is recommended to perform end trimming on special box-type fixtures reinforced with stiffening ribs, thereby significantly increasing the process's vibration resistance.

Acknowledgment

This contribution was supported by the European Union under the Program Slovakia (ITMS21+ code: 401101C504), the Ministry of Education, Research, Development, and Youth of the Slovak Republic (KEGA 012TUKE-4/2024, VEGA 1/0453/24), and the International Association for Technological Development and Innovations.

References

[1] Altintas, Y., Brecher, C., Weck, M., Witt, S. (2005). Virtual Machine Tool. *CIRP Annals*, 54(2), 115–138. https://doi.org/10.1016/S0007-8506(07)60022-5

[2] Erturk, A., Ozguven, H.N., Budak, E. (2006). Analytical modeling of spindle-tool dynamics on machine tools using Timoshenko beam theory and receptance coupling. *International Journal of Advanced Manufacturing Technology*, 28(7-8), 650–661. https://doi.org/10.1016/j.ijmachtools.2006.01.032

[3] Jablonski, W. (2010). Simulation of Cutting Process – Modeling and Applications. In: Dudas, L. (ed.) *Engineering the Future*. IntechOpen. http://dx.doi.org/10.5772/10374.

[4] Zhang, S., Li, J., Wang, S. (2019). Towards high milling accuracy of thin-walled parts: A review. *Mech. Syst. Signal Process*. 134, 106330.

[5] Li, W., Wang, L., Yu, G. (2021). Force-induced deformation prediction and flexible error compensation strategy in flank milling of thin-walled parts. *Journal of Materials Processing Technology,* 297, 117258. https://doi.org/10.1016/j.jmatprotec.2021.117258 .

[6] Kaymakci, M., Kilic, Z.M., Altintas, Y. (2012). Unified cutting force model for turning, boring, drilling, and milling operations. *International Journal of Machine Tools and Manufacture*, 54–55, 34–45. https://doi.org/10.1016/j.ijmachtools.2011.12.008.

[7] Moufki, A., Dudzinski, D., Le Coz, G. (2015). Prediction of cutting forces from an analytical model of oblique cutting, application to peripheral milling of Ti-6Al-4V alloy. *International Journal of Advanced Manufacturing Technology*, 81(1), 615–626. https://doi.org/10.1007/s00170-015-7018-1.

[8] Markopoulos, A.P. (2013). Finite Element Method in Machining Processes. *SpringerBriefs in Applied Sciences and Technology*. Springer, Heidelberg. https://doi.org/10.1007/978-1-4471-4330-7.

[9] Badovskyi, O., Balaniuk, A., Oborskyi, G., Orgiyan, A., Edl, M. (2024). An Increase in the Vibration Resistance of Finishing and Boring Machines when Cutting Ends Using the Plunge-In Method. In: Ivanov, V., Trojanowska, J., Pavlenko, I., Rauch, E., Pitel', J. (eds) *Advances in Design, Simulation and Manufacturing VII. DSMIE 2024. Lecture Notes in Mechanical Engineering* (pp. 139-151). Springer, Cham. https://doi.org/10.1007/978-3-031-61797-3_12.

[10] Qi, Z., Zhang, K., Cheng, H., Wang, D., Meng, Q. (2015). Microscopic mechanism-based force prediction in orthogonal cutting of unidirectional CFRP. *International Journal of Advanced Manufacturing Technology,* 79(5-8), 1209–1219. https://doi.org/10.1007/s00170-015-6895-7.

[11] Popovic, M.R., Tanovic, L., Ehmann, K.E. (2017). Cutting Forces Prediction: the Experimental Identification of Orthogonal Cutting Coefficients. *FME Transactions,* 45(4), 459–467. https://doi.org/10.5937/fmet1704459P.

[12] Adem, K.A.M., Fales, R., El-Gizawy, A.S. (2015). Identification of cutting force coefficients for the linear and nonlinear force models in the end milling process using average forces and optimization techniques. *International Journal of Advanced Manufacturing Technology*, 79(9-12), 1671–1687. https://doi.org/10.1007/s00170-015-6935-3.

[13] Hurey, I., Maruschak, P., Augousti, A., Flowers, A., Gurey, V., Dzyura, V., Prentkovskis, O. (2023). Resistance to Wear during Friction without Lubrication of Steel-Cast Iron Pairing with Nanocrystalline Structure-Reinforced Surface Layers. *Lubricants*, 11(10), 418 (2023). https://doi.org/10.3390/lubricants11100418.

[14] Banerjee, N., Sharma, A. (2016). Development of a friction model and its application in finite element analysis of minimum quantity lubrication machining of Ti-6Al-4V. *Journal of Materials Processing Technology*, 238, 181–194. https://doi.org/10.1016/j.jmatprotec.2016.07.017.

[15] Markopoulos, A.P., Karkalos, N.E., Vaxevanidis, N.M., Manolakos, D.E. (2016). Friction in Orthogonal Cutting Finite Elements Models with Large Negative Rake Angle. *Tribology in Industry*, 38(2), 214–220.

[16] Munoa, J., Beudaert, X., Dombovari, Z., Altintas, Y., Budak, E., Brecher, C., Stepan, G. (2016). Chatter suppression techniques in metal cutting. *CIRP Annals*, 65, 785–808. https://doi.org/10.1016/j.cirp.2016.06.004

[17] Sharma, V.S., Dhiman, S., Sehgal, R., et al. (2008). Estimation of cutting forces and surface roughness for hard turning using neural networks. *Journal of Intelligent Manufacturing*, 19, 473–483. https://doi.org/10.1007/s10845-008-0097-1.

[18] Alajmi, M.S., Alfares, F. (2007). Prediction of cutting forces in the turning process using Deep Neural Networks. In: *Proceedings of the 25th IASTED International Multi-Conference: Artificial Intelligence and Applications (pp. 41-46)*, Innsbruck.

[19] Karayel, D. (2009). Prediction and control of surface roughness in CNC lathe using an artificial neural network. *Journal of Materials Processing Technology*, 209, 3125–3137. https://doi.org/10.1016/j.jmatprotec.2008.07.023.

[20] Öktem, H. (2009). An integrated study of surface roughness for modeling and optimization of cutting parameters during end milling operation. *International Journal of Advanced Manufacturing Technology,* 43, 852–861. https://doi.org/10.1007/s00170-008-1763-3.

[21] Kunitsyn, M., Usov, A., Sikirash, Y. (2024). Mathematical Modeling of Thermomechanical Phenomena in the Machining of Products Made of Functionally Graded Materials. In: *Tonkonogyi, V., Ivanov, V., Trojanowska, J., Oborskyi, G., Pavlenko, I. (eds.) Advanced Manufacturing Processes V. InterPartner 2023. Lecture Notes in Mechanical Engineering* (pp. 60–72). Springer, Cham (2024). https://doi.org/10.1007/978-3-031-42778-7_6.

[22] Zheng, Q., Chen, G., Jiao, A. (2022). Chatter detection in the milling process based on the combination of wavelet packet transform and PSO-SVM. *International Journal of Advanced Manufacturing Technology,* 120, 1–15. https://doi.org/10.1007/s00170-022-08856-3.

[23] Ivchenko, O., et al. (2022). Method for an effective selection of tools and cutting conditions during precise turning of non-alloy quality steel C45. *Materials*, 15(2), 505. https://doi.org/10.3390/ma15020505.

[24] Hu, L., Cai, W., Shu, L., et al. (2021). Energy Optimisation for End Face Turning with Variable Material Removal Rate Considering the Spindle Speed Changes. *International Journal of Precision Engineering and Manufacturing-Green Technology*, 8, 625–638. https://doi.org/10.1007/s40684-020-00210-w.

[25] Saglam, H., Unsacar, F., Yaldiz, S. (2006). Investigation of the effect of rake angle and approaching angle on main cutting force and tool tip temperature. *International Journal of Machine Tools and Manufacture*, 46(2), 132–141. https://doi.org/10.1016/j.ijmachtools.2005.05.002.